Shock Waves in a Dusty Plasma with Positive and Negative Dust where Ions are Non-Thermal

Gurudas Mandal[a] and Prasanta Chatterjee[b,*]

[a] Department of ECE, East West University Mohakhali, Dhaka-1212, Bangladesh
[b] Plasma Physics Laboratory, Department of Physics, University of Malaya, Malaysia
[*] On leave from the Department of Mathematics, Visva Bharati University, Santiniketan, India

Reprint requests to G. M.; Fax: +880 28812336; E-mail: gdmandal@ewubd.edu

Z. Naturforsch. **65a,** 85 – 90 (2010); received March 3, 2009

A four-component dusty plasma consisting of electrons, ions, and negatively as well as positively charged dust grains has been considered. Shock waves may exist in such a four-component dusty plasma. The basic characteristics of shock waves have been theoretically investigated by employing reductive perturbation technique (RPT). It is found that negative as well as positive shock potentials are present in such dusty plasma. The present results may be useful for understanding the existence of nonlinear potential structures that are observed in different regions of space (viz. cometary tails, lower and upper mesosphere, Jupiter's magnetosphere, interstellar media, etc).

Key words: Dusty Plasma; Shock Waves; Non-Thermal; Dust Acoustic (DA) Wave.

1. Introduction

The nonlinear behaviour of charged dust particles has received much attention in the recent years because of its vital role in understanding of electrostatic density perturbations and nonlinear potential structures which are observed in different regions of space environments, namely lower and upper mesosphere, cometary tails, planetary rings, planetary magnetosphere, interplanetary space, interstellar media, etc. [1 – 4]. Most of the dusty plasma studies have been confined in considering that the dust grains are negatively charged [5 – 11]. Very recent it has been found that there are some plasma systems, particularly in space plasma environment, where positively charged dust grains are present and also play a significant role [2, 3, 12, 13]. There are three basic mechanisms by which the dust grains in the plasma system mentioned above can be positively charged [14]. These three mechanisms are the following: (i) photoemission in the presence of a flux of ultraviolet (UV) photons, (ii) thermionic emission induced by radiative heating, and (iii) secondary emission of electrons from the surface of the dust grains.

Chow et al. [12] have shown theoretically that due to the size effect on secondary emission insulating dust grains with different sizes in space plasmas can have the opposite polarity (smaller ones being positive and larger ones being negative). This is mainly due to the fact that the excited secondary electrons have shorter (longer) distance to travel to reach the surface of the smaller (larger) dust grains [12].

There are also direct evidences for the existence of both positively and negatively charged dust particles in different regions of space, viz. cometary tails [2, 3, 12], upper mesosphere [13], Jupiter's magnetosphere [15], etc. It has been suggested that the coexistence of positively and negatively charged dust are also present in laboratory plasmas [2, 3, 16]. On basis of theoretical predictions and satellite observations, Mamun and Shukla [17] have considered a very simple dusty plasma system, which assumes positively and negatively charged dust particles only, and have theoretically investigated the properties of linear/nonlinear electrostatic waves that may propagate in such a dusty plasma system. This simple system is only valid if a complete depletion of background electrons and ions in the dusty plasma is considered. However, a complete depletion of background electrons and ions in most of the cases is not possible. Recently, Armina et al. [18] have considered a four-component dusty plasma containing positively and negatively charged dust and Boltzmann distributed electrons and ions. They have investigated the possibility for the formation of shock waves and also found the existence shock structures in this four-component dusty plasma. Recent observations [19, 20] show that the ion distribution does not follow a Boltzmann distribution and in

these cases the non-thermal distribution of ions is suggested.

In our present work, we considered a four-component unmagnetized dusty plasma system containing Boltzmann distributed electrons, non-thermal distributed ions, and also positively (smaller size) and negatively (larger size) charged dust grains.

The manuscript is organized as follows: The basic equations governing the dusty plasma system are presented in Section 2. The nonlinear Burgers equation for the propagation of dust acoustic (DA) shock waves is derived in Section 3. The stationary shock wave solution of the Burgers equation is analyzed in Section 4. Finally, a brief discussion is presented in Section 5.

2. Governing Equations

We consider a one-dimensional (1D), unmagnetized collision less dusty plasma consisting of Boltzmann distributed electrons, non-thermal distributed ions, and positively and negatively charged dust grains. The nonlinear dynamics of DA waves is governed by

$$\frac{\partial n_1}{\partial t}+\frac{\partial}{\partial x}(n_1u_1)=0, \tag{1}$$

$$\frac{\partial u_1}{\partial t}+u_1\frac{\partial u_1}{\partial x}=\frac{z_1e}{m_1}\cdot\frac{\partial\phi}{\partial x}+\eta_{\mathrm{I}}\frac{\partial^2u_1}{\partial x^2}, \tag{2}$$

$$\frac{\partial n_2}{\partial t}+\frac{\partial}{\partial x}(n_2u_2)=0, \tag{3}$$

$$\frac{\partial u_2}{\partial t}+u_2\frac{\partial u_2}{\partial x}=-\frac{z_2e}{m_2}\cdot\frac{\partial\phi}{\partial x}+\eta_{\mathrm{II}}\frac{\partial^2u_2}{\partial x^2}, \tag{4}$$

$$n_{\mathrm{e}}-n_{\mathrm{i}}+z_1n_1-z_2n_2=0, \tag{5}$$

where $n_1(n_2)$ is the negative (positive) dust number density, $u_1(u_2)$ is the negative (positive) dust fluid speed, $z_1(z_2)$ is the number of electrons (protons) residing on a negative (positive) dust particles, $m_1(m_2)$ is the mass of negative (positive) dust particle, $-e$ is the electronic charge, ϕ is the wave potential, $\eta_{\mathrm{I}}(\eta_{\mathrm{II}})$ is the viscosity coefficient of negative (positive) dust fluid, x is the space variable, and t is the time variable. $n_{\mathrm{e}}(n_{\mathrm{i}})$ is the electron (ion) number density: $n_{\mathrm{e}}=n_{\mathrm{e0}}\mathrm{e}^{\frac{e\phi}{k_{\mathrm{B}}T_{\mathrm{e}}}}$, $n_{\mathrm{i}}=n_{\mathrm{i0}}\Big[1+\beta_1\left(\frac{e\phi}{k_{\mathrm{B}}T_{\mathrm{i}}}\right)+\beta_1\left(\frac{e\phi}{k_{\mathrm{B}}T_{\mathrm{i}}}\right)^2\Big]\mathrm{e}^{-\left(\frac{e\phi}{k_{\mathrm{B}}T_{\mathrm{e}}}\right)}$, $\beta_1=\frac{4\alpha_1}{1+3\alpha_1}$, α_1 is the non-thermal parameter that determines the number of fast ions, $T_{\mathrm{e}(T_{\mathrm{i}})}$ is the temperature of electrons (ions), and k_{B} is the Boltzmann constant. In (5) we have assumed the quasi-neutrality condition at equilibrium. Now, in terms of normalized variables, namely $N_1=\frac{n_1}{n_{10}}$, $N_2=\frac{n_2}{n_{20}}$, $U_1=\frac{u_1}{C_1}$, $U_2=\frac{u_2}{C_1}$, $\psi=\frac{e\phi}{k_{\mathrm{B}}T_{\mathrm{i}}}$, $T=t\omega_{\mathrm{pd}}$, $X=\frac{x}{\lambda_{\mathrm{D}}}$, $\eta_1=\eta_{\mathrm{I}}\omega_{\mathrm{pd}}{\lambda_{\mathrm{D}}}^2$, $\eta_2=\eta_{\mathrm{II}}\omega_{\mathrm{pd}}{\lambda_{\mathrm{D}}}^2$, where $n_{10}(n_{20})$ is equilibrium value of $n_1(n_2)$, $C_1=\sqrt{\frac{z_1k_{\mathrm{B}}T_{\mathrm{i}}}{m_1}}$, $\omega_{\mathrm{pd}}=\sqrt{\frac{4\pi{z_1}^2e^2n_{10}}{m_1}}$, and $\lambda_{\mathrm{D}}=\sqrt{\frac{z_1k_{\mathrm{B}}T_{\mathrm{i}}}{4\pi{z_1}^2e^2n_{10}}}$. We can express (1) – (5) as

$$\frac{\partial N_1}{\partial T}+\frac{\partial}{\partial X}(N_1U_1)=0, \tag{6}$$

$$\frac{\partial U_1}{\partial T}+U_1\frac{\partial U_1}{\partial X}=\frac{\partial\psi}{\partial X}+\eta_1\frac{\partial^2U_1}{\partial X^2}, \tag{7}$$

$$\frac{\partial N_2}{\partial T}+\frac{\partial}{\partial X}(N_2U_2)=0, \tag{8}$$

$$\frac{\partial U_2}{\partial T}+U_2\frac{\partial U_2}{\partial X}=-\alpha\beta\frac{\partial\psi}{\partial X}+\eta_2\frac{\partial^2U_2}{\partial X^2}, \tag{9}$$

$$\begin{aligned}N_1=(1+\mu_{\mathrm{e}}-\mu_{\mathrm{i}})N_2-\mu_{\mathrm{e}}\mathrm{e}^{\sigma\psi}\\+\mu_{\mathrm{i}}(1+\beta_1\psi+\beta_1\psi^2)\mathrm{e}^{-\psi},\end{aligned} \tag{10}$$

where $\alpha=\frac{z_2}{z_1}$, $\beta=\frac{m_1}{m_2}$, $\mu_{\mathrm{e}}=\frac{n_{\mathrm{e0}}}{z_1n_{10}}$, $\mu_{\mathrm{i}}=\frac{n_{\mathrm{i0}}}{z_1n_{10}}$, and $\sigma=\frac{T_{\mathrm{i}}}{T_{\mathrm{e}}}$.

3. Derivation of Burgers Equation

Now, we derive the Burgers equation from (6) – (10) by employing the reductive perturbation technique (RPT) and the stretch coordinates [21] $\xi=\varepsilon^{1/2}(X-V_0T)$, and $\tau=\varepsilon^{3/2}T$, where ε is a smallness parameter measuring the weakness of the nonlinearity and V_0 is phase speed of the DA waves normalized by C_1. We now express (6) – (10) in terms of ξ and τ as

$$\varepsilon^{3/2}\frac{\partial N_1}{\partial\tau}-V_0\varepsilon^{1/2}\frac{\partial N_1}{\partial\xi}+\varepsilon^{1/2}\frac{\partial}{\partial\xi}(N_1U_1)=0, \tag{11}$$

$$\begin{aligned}\varepsilon^{3/2}\frac{\partial U_1}{\partial\tau}-V_0\varepsilon^{1/2}\frac{\partial U_1}{\partial\xi}+\varepsilon^{1/2}U_1\frac{\partial U_1}{\partial\xi}=\\\varepsilon^{1/2}\frac{\partial\psi}{\partial\tau}+\varepsilon^{3/2}\eta_{10}\frac{\partial^2U_1}{\partial\xi^2},\end{aligned} \tag{12}$$

$$\varepsilon^{3/2}\frac{\partial N_2}{\partial\tau}-V_0\varepsilon^{1/2}\frac{\partial N_2}{\partial\xi}+\varepsilon^{1/2}\frac{\partial}{\partial\xi}(N_2U_2)=0, \tag{13}$$

$$\begin{aligned}\varepsilon^{3/2}\frac{\partial U_2}{\partial\tau}-V_0\varepsilon^{1/2}\frac{\partial U_2}{\partial\xi}+\varepsilon^{1/2}U_2\frac{\partial U_2}{\partial\xi}=\\-\varepsilon^{1/2}\alpha\beta\frac{\partial\psi}{\partial\tau}+\varepsilon^{3/2}\eta_{20}\frac{\partial^2U_2}{\partial\xi^2},\end{aligned} \tag{14}$$

$$N_1 = (1+\mu_e-\mu_i)N_2 - \mu_e e^{\sigma\psi} + \mu_i(1+\beta_1\psi+\beta_1\psi^2)e^{-\psi}, \quad (15)$$

where $\eta_1 = \varepsilon^{1/2}\eta_{10}$ and $\eta_2 = \varepsilon^{1/2}\eta_{20}$ are assumed [17].

We can expand the variables N_1, U_1, N_2, U_2, and ψ in a power series of ε as

$$N_1 = 1+\varepsilon N_1^{(1)} + \varepsilon^2 N_1^{(2)} + \ldots, \quad (16)$$

$$U_1 = 0+\varepsilon U_1^{(1)} + \varepsilon^2 U_1^{(2)} + \ldots, \quad (17)$$

$$N_2 = 1+\varepsilon N_2^{(1)} + \varepsilon^2 N_2^{(2)} + \ldots, \quad (18)$$

$$U_2 = 0+\varepsilon U_2^{(1)} + \varepsilon^2 U_2^{(2)} + \ldots, \quad (19)$$

$$\psi = 0+\varepsilon\psi^{(1)} + \varepsilon^2\psi^{(2)} + \ldots. \quad (20)$$

Now, substituting (16)–(20) into (11)–(15) and taking the coefficient of $\varepsilon^{3/2}$ from (11)–(14) and ε from (15) we have

$$N_1^{(1)} = \frac{U_1^{(1)}}{V_0}, \quad (21)$$

$$U_1^{(1)} = -\frac{\psi^{(1)}}{V_0}, \quad (22)$$

$$N_2^{(1)} = \frac{U_2^{(1)}}{V_0}, \quad (23)$$

$$U_2^{(1)} = (\alpha\beta)\frac{\psi^{(1)}}{V_0}, \quad (24)$$

$$N_1^{(1)} = (1+\mu_e-\mu_i)N_2^{(1)} - \mu_e\sigma\psi^{(1)} + \mu_i\beta_1\psi^{(1)}. \quad (25)$$

Now, using (21)–(25) we get

$$N_1^{(1)} = -\frac{\psi^{(1)}}{V_0^2}, \quad (26)$$

$$N_2^{(1)} = (\alpha\beta)\frac{\psi^{(1)}}{V_0^2}, \quad (27)$$

$$V_0^2 = \frac{1+\alpha\beta(1+\mu_e-\mu_i)}{\sigma\mu_e-\mu_i\beta_1}. \quad (28)$$

(28) is the linear dispersion relation for the DA waves propagating in our dusty plasma system. Similarly, substituting (16)–(20) into (11)–(15) and equating the coefficient of $\varepsilon^{5/2}$ from (11)–(14) and ε^2 from (15) one obtains

$$\frac{\partial N_1^{(1)}}{\partial\tau} - V_0\frac{\partial N_1^{(2)}}{\partial\xi} + \frac{\partial U_1^{(2)}}{\partial\xi} + \frac{\partial}{\partial\xi}[N_1^{(1)}U_1^{(1)}] = 0, \quad (29)$$

$$\frac{\partial U_1^{(1)}}{\partial\tau} - V_0\frac{\partial U_1^{(2)}}{\partial\xi} + U_1^{(1)}\frac{\partial U_1^{(1)}}{\partial\xi} = \frac{\partial\psi^{(2)}}{\partial\xi} + \eta_{10}\frac{\partial^2 U_1^{(1)}}{\partial\xi^2}, \quad (30)$$

$$\frac{\partial N_2^{(1)}}{\partial\tau} - V_0\frac{\partial N_2^{(2)}}{\partial\xi} + \frac{\partial U_2^{(2)}}{\partial\xi} + \frac{\partial}{\partial\xi}[N_2^{(1)}U_2^{(1)}] = 0, \quad (31)$$

$$\frac{\partial U_2^{(1)}}{\partial\tau} - V_0\frac{\partial U_2^{(2)}}{\partial\xi} + U_2^{(1)}\frac{\partial U_2^{(1)}}{\partial\xi} = -\alpha\beta\frac{\partial\psi^{(2)}}{\partial\xi} + \eta_{20}\frac{\partial^2 U_2^{(1)}}{\partial\xi^2}, \quad (32)$$

$$N_1^{(2)} = (1+\mu_e-\mu_i)N_2^{(2)} - \mu_e\sigma\psi^{(2)} - \frac{1}{2}\sigma^2\mu_e[\psi^{(1)}]^2 + \mu_i\beta_1\psi^{(2)} + \mu_i\beta_1[\psi^{(1)}]^2. \quad (33)$$

Now, using (22), (24), and (26)–(28), and eliminating $N_1^{(2)}$, $N_2^{(2)}$, $U_1^{(2)}$, $U_2^{(2)}$, and $\psi^{(2)}$, we finally obtain

$$\frac{\partial\psi^{(1)}}{\partial\tau} + A\psi^{(1)}\frac{\partial\psi^{(1)}}{\partial\xi} = C\frac{\partial^2\psi^{(1)}}{\partial\xi^2}, \quad (34)$$

where the nonlinear coefficient A and the dissipation coefficient C are given by

$$A = \frac{3\alpha^2\beta^2(1+\mu_e-\mu_i) - 3 - V_0^4(\sigma^2\mu_e - 2\mu_i\beta_1)}{2V_0[1+\alpha\beta(1+\mu_e-\mu_i)]}, \quad (35)$$

$$C = \frac{\eta_{10}+\alpha\beta\eta_{20}}{2[1+\alpha\beta(1+\mu_e-\mu_i)]}. \quad (36)$$

(34) is known as Burgers equation which can describe the nonlinear propagation of DA waves in our four-component dusty plasma system.

4. Solution of Burgers Equation

The stationary solution of this Burgers equation is obtained by transforming the independent variables ξ and τ to $\zeta = \xi - U_0\tau$ and $\tau = \tau$, where U_0 is a constant velocity normalized by C_1, and imposing the appropriate boundary conditions, viz. $\psi^{(1)} \to 0$, $\frac{\partial\psi^{(1)}}{\partial\zeta} \to 0$, at $\zeta \to \infty$. Thus, one can express the stationary solution of the Burgers equation as

$$\psi^{(1)} = \psi_m^{(1)}[1 - \tanh(\zeta/\Delta)], \quad (37)$$

where the amplitude $\psi_m^{(1)}$ (normalized by $k_B T_i/e$) and the width Δ (normalized by λ_D) are given by

$$\psi_m^{(1)} = \frac{U_0}{A}, \quad (38)$$

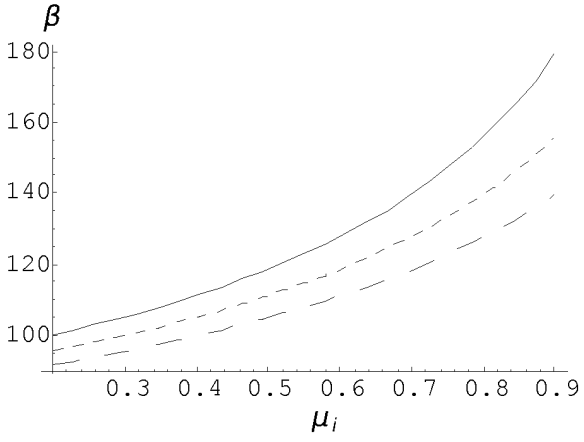

Fig. 1. $A = 0$ (β vs. μ_i) curves for $\alpha = 0.01$, $\sigma = 0.5$, $\mu_e = 0.2$ (solid curve), $\mu_e = 0.3$ (dotted curve), $\mu_e = 0.4$ (dashed curve).

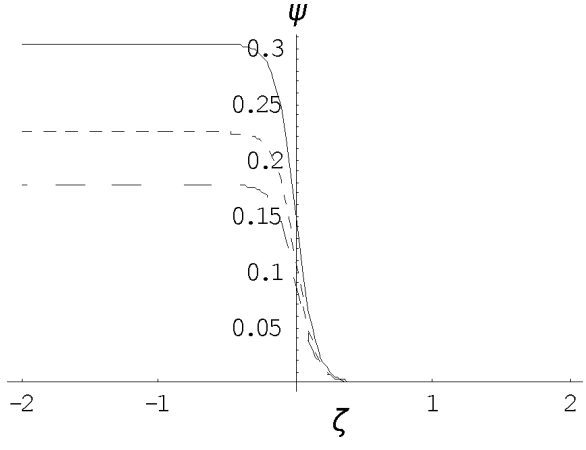

Fig. 2. Positive shock potential profiles (ψ vs. ζ curves) for $\alpha = 0.01$, $\sigma = 0.5$, $\mu_i = 0.5$, $\mu_e = 0.3$, $\eta_{10} = 0.1$, $\eta_{20} = 0.1$ $\beta = 400$ (solid curve), $\beta = 500$ (dotted curve), $\beta = 600$ (dashed curve).

$$\Delta = \frac{2C}{U_0}. \tag{39}$$

It is observed from (37)–(39) that the amplitude (width) of the shock waves increases (decreases) as U_0 increases. It is also clear from (35), (37), and (38) that shock potential profile is positive (negative) when A is positive (negative). To find the different range of values of β and μ_i for which the positive and negative potential profiles exist, we obtain $A = 0$ (β vs. μ_i) curves. The $A = 0$ (β vs. μ_i) curves are displayed in Figure 1. From these $A = 0$ curves, we can have positive (negative) shock potential profiles for the parameters whose values lie above (below) the curves.

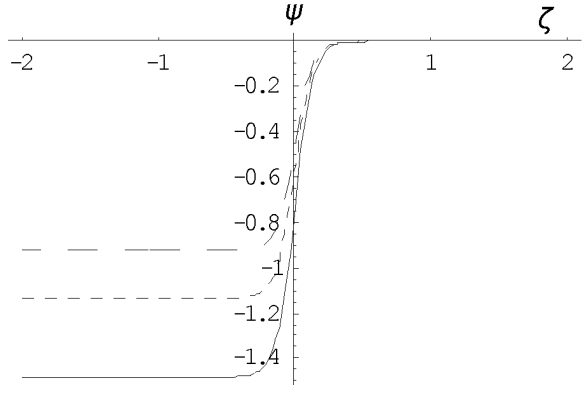

Fig. 3. Negative shock potential profiles (ψ vs. ζ curves) for $\alpha = 0.01$, $\sigma = 0.5$, $\mu_i = 0.5$, $\mu_e = 0.3$, $\eta_{10} = 0.1$, $\eta_{20} = 0.1$ $\beta = 50$ (solid curve), $\beta = 40$ (dotted curve), $\beta = 30$ (dashed curve).

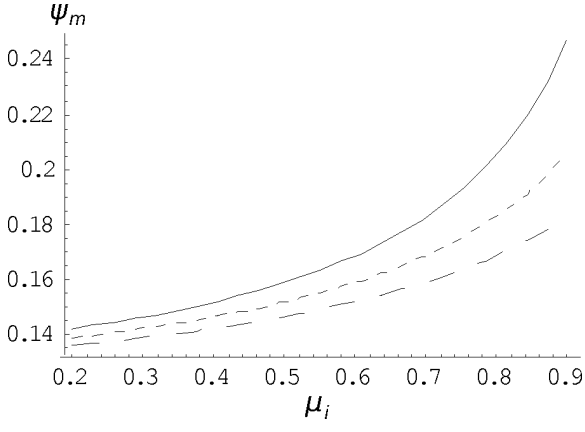

Fig. 4. Positive amplitude profiles (ψ_m vs. μ_i curves) for $\alpha = 0.01$, $\sigma = 0.5$, $\beta = 400$, $\eta_{10} = 0.1$, $\eta_{20} = 0.1$, $\mu_e = 0.2$ (solid curve), $\mu_e = 0.3$ (dotted curve), $\mu_e = 0.4$ (dashed curve).

Figure 2 and Figure 3 show how positive and negative shock potentials vary with β. Figure 2 shows the positive shock potential profile, where the potential decreases with the increase of β. Figure 3 shows the negative shock potential profile, where the potential decreases with decrease of β. Figure 4 and Figure 5 show the positive (negative) amplitude (ψ_m) profiles of shock waves and how it varies with μ_e. Figure 4, for the positive amplitude profile shows that the amplitude of the shock waves increases as μ_e increases. Figure 5, for the negative amplitude profile shows that the amplitude of shock waves decreases as μ_e increases. Figure 6 and Figure 7 show how the width of shock waves varies ($\beta = 400$ for Fig. 6 and $\beta = 40$ for Fig. 7) with μ_e. For both the values of β, the width (Δ) of shock waves always decreases as μ_e increases.

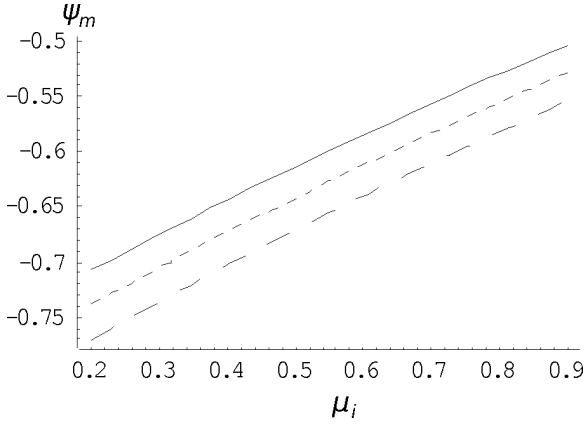

Fig. 5. Negative amplitude profiles (ψ_m vs. μ_i curves) for $\alpha = 0.01$, $\sigma = 0.5$, $\beta = 40$, $\eta_{10} = 0.1$, $\eta_{20} = 0.1$, $\mu_e = 0.2$ (solid curve), $\mu_e = 0.3$ (dotted curve), $\mu_e = 0.4$ (dashed curve).

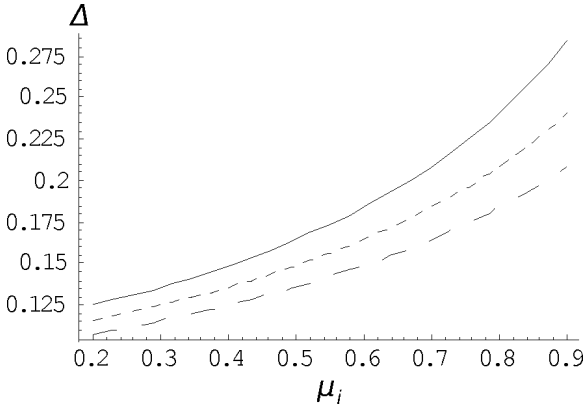

Fig. 6. Width profile (Δ vs. μ_i curves) for $\alpha = 0.01$, $\sigma = 0.5$, $\beta = 400$, $\eta_{10} = 0.1$, $\eta_{20} = 0.1$, $\mu_e = 0.2$ (solid curve), $\mu_e = 0.3$ (dotted curve), $\mu_e = 0.4$ (dashed curve).

5. Discussion

We have considered unmagnetized dusty plasma containing mobile positive and negative charged dust, Boltzmann electrons, and non-thermal distributed ions, and have theoretically investigated the basic features of the DA shock waves by employing the reductive perturbation technique (RPT). It has been found in (35) that if we consider there is no positive dust grains in the plasma system, i. e. $z_2 = 0$, hence $\alpha = 0$ then A is always negative. It indicates only the existence of negative shock potentials in the plasma system. We have then investigated the effect of coexistence of positive and negative dust grains, and we found that after certain values of α and β (which corresponds to the presence of certain number of positive dust), one can have positive shock potential structures in the dusty plasma system. Armina et al. [18] found the similar result though they have considered the plasma system containing positive and negative dust grains, Boltzmann electrons and ions. The following features have been noticed in this theoretical investigation: (i) the amplitude of both the positive and negative shock potential structures increases with increasing of U_0, (ii) the width of both the positive and negative shock potential structures decreases with increasing of U_0, (iii) the positive and negative shock potentials are almost doubled when ion distribution is considered as non-thermal instead of Boltzmann ions [18], (iv) the potential of the positive shock structures decreases with increasing of β, (v) the potential of the negative shock structures increases with increasing of β, (vi) the amplitude and the width of the DA shock waves are positive for $\beta = 400$ and both are decreasing with increasing of μ_e, (vii) the amplitude of the DA shock waves is negative for $\beta = 40$ and is increasing with increasing of μ_e, and (viii) the width of the DA shock waves is also decreasing for $\beta = 40$ with increasing of μ_e.

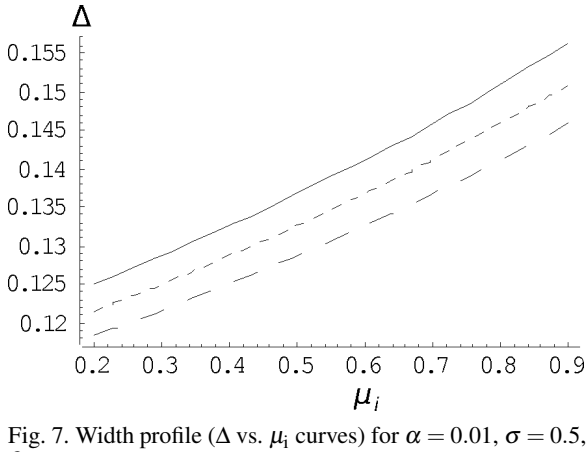

Fig. 7. Width profile (Δ vs. μ_i curves) for $\alpha = 0.01$, $\sigma = 0.5$, $\beta = 40$, $\eta_{10} = 0.1$, $\eta_{20} = 0.1$, $\mu_e = 0.2$ (solid curve), $\mu_e = 0.3$ (dotted curve), $\mu_e = 0.4$ (dashed curve).

It would be possible that the shock negative potential may trap positively charged dust particles which can attract dust particles of opposite polarity to form larger sized dust or to be coagulated into extremely large sized neutral dust in cometary tails, upper mesosphere, Jupiter's magnetosphere or even in laboratory experiments.

The parameters chosen in our numerical calculations are completely relevant to different regions of

space, viz. cometary tails [2, 3, 12], mesosphere [13]; Jupiter's magnetosphere [15], etc. In conclusion, we stress that our theoretical investigation and results may also be applied to laboratory dusty plasma devices which will be able to produce a plasma containing positive and negative dust grains.

[1] M. Horanyi and D. A. Mendis, J. Geophys. Res. **91**, 355 (1986).
[2] D. A. Mendis and M. Rosenberg, Annu. Rev. Astron. Astrophys. **32**, 419 (1994).
[3] M. Horanyi, Annu. Rev. Astron. Astrophys, **34**, 383 (1996).
[4] P. K. Shukla and A. A. Mamun, Introduction to Dust Plasma Physics, IoP Publishing Ltd., Bristol 2002.
[5] N. N. Rao, P. K. Shukla, and M. Y. Yu, Planet. Space Sci. **38**, 543 (1990).
[6] J. X. Ma and L. Liu, Phys. Plasmas **4**, 253 (1997).
[7] A. A. Mamun, Phys. Scripta **57**, 258 (1998).
[8] A. A. Mamun, Astrophys. Space Sci. **268**, 443 (1999).
[9] A. A. Mamun and P. K. Shukla, Phys. Lett. A **290**, 173 (2001).
[10] W. M. Moslem, Phys. Plasmas **10**, 3168 (2003).
[11] J. K. Xue, Phys. Rev. E **69**, 016403 (2004).
[12] V. W. Chow., D. A. Mendis, and M. Rosenberg, J. Geophys. Res. **98**, 19065 (1993).
[13] O. Havnes, J. Trøim, T. Blix, W. Mortensen, L. I. Naesheim, E. Thrane, and T. Tønnesen, J. Geophys. Res. **101**, 1039 (1996).
[14] V. E. Fortov, A. P. Nefedov, and O. S. Vaulina, J. Exp. Theor. Phys. **87**, 1087 (1998).
[15] M. Horanyi, G. E. Morfill, and E. Grtin, Nature **363**, l44 (1993).
[16] D. A. Mendis and M. Horanyi, in Cometary Plasma Processes, AGU Monograph **61**, 17 (1991).
[17] A. A. Mamun and P. K. Shukla, Geophys. Rev. Lett. **29**, 1870 (2002).
[18] R. Armina, A. A. Mamun, and S. M. K. Alam, Astrophys. Space Sci. **315**, 243 (2008).
[19] R. Lundlin, A. Zakharov, R. Pelinenn, B. Hultqvist, H. Borg, E. M. Dubinin, S. Barabasj, N. Pissarenkon, H. Koskinen, and I. Liede, Nature **341**, 609 (1989).
[20] Y. Futaana, S. Machida, Y. Saito, A. Matsuoka, and H. Hayakawa, J. Geophys. Res. **108**, 151 (2003).
[21] H. Washimi and T. Taniuti, Phys. Rev. Lett. **17**, 996 (1966).